Signal Quality Assessment and Lightweight QRS Detection for Wearable ECG SmartVest System

Chengyu Liu, *Member, IEEE*, Xiangyu Zhang, Lina Zhao, Feifei Liu, Xingwen Chen, Yingjia Yao, and Jianqing Li, *Member, IEEE*

***Abstract*—Recently, development of wearable and Internet of Things (IoT) technologies enables the real-time and continuous individual electrocardiogram (ECG) monitoring. In this paper, we develop a novel IoT-based wearable 12-lead ECG SmartVest system for early detection of cardiovascular diseases, which consists of four typical IoT components: 1) sensing layer using textile dry ECG electrode; 2) network layer utilizing Bluetooth, WiFi, etc.; 3) cloud saving and calculation platform and server; and 4) application layer for signal analysis and decision making. We focus on addressing the challenge of real-time signal quality assessment (SQA) and lightweight QRS detection for wearable ECG application. First, a combination method of multiple signal quality indices and machine learning is proposed for classifying 10-s single-channel ECG segments as acceptable and unacceptable. Then a lightweight QRS detector is developed for accurate location of QRS complexes. The results show that the proposed SQA method can efficiently deal with tradeoff between accepting good (97.9%) and rejecting poor (96.4%) quality ECGs, ensuring that only a low percentage of recorded ECGs are discarded. The proposed lightweight QRS detector achieves a F_1 score higher than 99.5% for processing clean ECGs. Meanwhile, it reports significantly higher F_1 scores than two existing QRS detectors for processing noisy ECGs. In addition, it also has a fine computation efficiency. This paper demonstrates that the developed IoT-driven ECG SmartVest system can be applied for widely monitoring the population during daily life and has a promising application future.**

***Index Terms*—Cardiovascular disease (CVD) monitoring, eHealth and mHealth, electrocardiogram (ECG), electrocardiogram QRS detection, Internet of Things (IoT), signal quality assessment (SQA), wearable ECG device.**

Manuscript received January 15, 2018; revised May 1, 2018; accepted May 27, 2018. Date of publication June 4, 2018; date of current version May 8, 2019. This work was supported in part by the National Natural Science Foundation of China under Grant 61571113 and Grant 61671275, in part by the Key Research and Development Programs of Jiangsu Province under Grant BE2017735, in part by the Fundamental Research Funds for the Central Universities under Grant 2242018k1G010, and in part by the Southeast-Lenovo Wearable Heart-Sleep-Emotion Intelligent Monitoring Laboratory. *(Corresponding authors: Chengyu Liu; Jianqing Li.)*

C. Liu, X. Zhang, and F. Liu are with the State Key Laboratory of Bioelectronics, Jiangsu Key Laboratory of Remote Measurement and Control, School of Instrument Science and Engineering, Southeast University, Nanjing 210096, China (e-mail: chengyu@seu.edu.cn; 230179249@seu.edu.cn; feifeiliu1987@gmail.com).

L. Zhao is with the State Key Laboratory of Bioelectronics, Jiangsu Key Laboratory of Remote Measurement and Control, School of Instrument Science and Engineering, Southeast University, Nanjing 210096, China, and also with the School of Control Science and Engineering, Shandong University, Jinan, 250061, China (e-mail: zhaolina0808@126.com).

X. Chen is with the Lenovo China Empowerment Center, Lenovo, Shenzhen 518057, China (e-mail: chenxwd@lenovo.com).

Y. Yao is with the Lenovo China Empowerment Center, Lenovo, Beijing 100085, China (e-mail: yaoyj@lenovo.com).

J. Li is with the State Key Laboratory of Bioelectronics, Jiangsu Key Laboratory of Remote Measurement and Control, the School of Instrument Science and Engineering, Southeast University, Nanjing 210096, China, and also with the School of Basic Medical Sciences, Nanjing Medical University, Nanjing 211166, China (e-mail: ljq@seu.edu.cn).

Digital Object Identifier 10.1109/JIOT.2018.2844090

I. Introduction

Cardiovascular diseases (CVDs) are the leading cause of death globally (32.1%) and result in 17.9 million deaths in 2015 [1]. However, it is estimated that 90% of CVDs is preventable [2]. The sooner the disease is detected, the better quality of life the patient will have. Electrocardiogram (ECG) is a good way for early monitoring of CVDs; however, traditional clinical ECG scan only includes limited time length signals, missing the asymptomatic or intermittent characteristics of CVDs. Therefore, developing real-time, long-term ECG monitoring is essential for disease early detection. Thanks to the quick development of wearable and Internet of Things (IoT) technologies, making the real-time, long-term, and convenient individual ECG monitoring available [3]–[6].

The IoT-driven ECG monitoring can play a significant role in improving the health and wellness of subjects by increasing the availability and quality of healthcare, with the application for CVD early detection, as well as for other situations, such as sports and fitness, rehabilitation, elderly care support, emotion and sleep monitoring, etc. [4], [7], [8]. Meanwhile, it can significantly reduce travel, cost and time in remote and long-term ECG monitoring [7]–[9]. However, for IoT-driven wearable ECG monitoring, technology challenges exist, and are mainly from the following aspects.

The first challenge comes from the physical implementation (hardware) of the wearable smart ECG garment system, including textile sensor design [10], ergonomic design for comfort measurement [11], [12], wireless transmission [13], power consumption and optimization [14].

The second comes from the real-time and accurate signal analysis performed on the embedded processor in smartphone, including signal quality assessment (SQA), real-time and adaptive feature extraction, intelligent diagnosis for ECG abnormalities (both rhythm and morphology abnormalities).

SQA is an essential step for the intelligent ECG analysis. ECGs collected via mobile approach are easily polluted by a variety of noises, including body movement,

2327-4662 © 2018 IEEE. Personal use is permitted, but republication/redistribution requires IEEE permission.
See http://www.ieee.org/publications_standards/publications/rights/index.html for more information.

circumstance interference, etc. [15], [16]. The corrupted ECG data could lead to medical misdiagnosis via cardiac monitors. SQA has been a research topic since the success of the physionet/computing in cardiology challenge 2011 [16], [17], which generated a lot of advanced method for SQA. The typical methods include: threshold-based [18], multifeature fusion [19], ensemble decision trees [20], self-organizing neural network [21], regularity matrix [22], combination of signal quality indices (SQIs) and support vector machine (SVM) [15], [16].

QRS complex is the most striking waveform and it serves as the basis for the automated determination of other ECG characteristics. QRS detection has been extensively studied for over 40 years. The typical methods include: Pan-Tompkins (P&T) algorithm [23] and its variations [24], [25], RS-Slope method [26], adaptive wavelet multiresolution analysis [27], difference operation method [28], max–min difference method [29], optimized knowledge based algorithm [30], Fourier and Hilbert transforms [31], *wqrs* algorithm [32], etc. Currently, the accuracy of QRS detector for processing noisy wearable ECGs need to be improved. Portable battery-operated devices have limited computation resource. Thus improvement of computation cost efficient is also necessary.

The third comes from the big data processing, machine learning, and cloud computing for long-term ECG big data analysis, which involves the determination of efficient machine learning methods [33], [34], long-term prediction and inference methods for disease risk evaluation, deep-learning, and deep-mining for specific disease type.

In this paper, we first described the system architecture for the developed Wearable 12-lead ECG SmartVest system. Then we focused on the key SQA and QRS detection for single-channel ECG processing used in the smartphone-side of the developed device. We aimed to present a real-time and lightweight single-channel ECG processing scheme for use of IoT-driven wearable devices and reducing the burden in cloud server, and identified two key contributions as follows.

1) SQA methods from analyzing good quality ECGs are not suitable for wearable ECG analysis. For wearable ECG monitoring, the majority of ECGs have a variety of noise components. So intelligent SQA method should automatically identify the ECG episodes, although noisy but with diagnosis value, as the "acceptable." This is the first contribution.
2) Textile dry electrodes were used in SmartVest to replace the Ag/AgCl electrodes. Relative displacement changes between the electrode and skin can induce large amplitude and unexpected noises. ECGs recorded by SmartVest tend to be more vulnerable to noises. Thus accurate QRS detection is challenging. So the second contribution is to develop a robust and lightweight QRS detector to adaptively and intelligently detect the QRS complexes under complicated noisy environment.

This paper is organized as follows. Section II briefly summarizes the system architecture for the developed ECG SmartVest system. Section III details the methods of SQA and lightweight QRS detection. Section IV presents the experiment designs, including the data and evaluation approaches. Section V details the results. Section VI gives the discussions. Finally, Section VII summarizes the conclusion.

II. Architecture of Wearable 12-Lead ECG SmartVest System

In this section, we present the architecture of the wearable 12-lead ECG SmartVest system, which provides an IoT-driven 24/7 ECG monitoring service for people that may have potential CVD risks. As illustrated in Fig. 1, the IoT-driven based system consists of four typical IoT components, i.e., sensing layer, network layer, cloud platform, and application layer.

In sensing layer, individual multichannel ECGs are simultaneously collected using ten textile dry electrodes embedded in the SmartVest. Four electrodes (RA, LA, LL, and RL) are attached in the four corners of torso, and six electrodes (V1, V2, V3, V4, V5, and V6) are attached on the chest. The collected multichannel ECGs are common 12-lead ECGs, namely as I, II, III, aVR, aVL, aVF, V1, V2, V3, V4, V5, and V6. Using of conductive textile electrodes is to meet the comfort requirement. A self-charged ECG module is embedded in SmartVest, which can start-up signal recording, and implement hardware filtering, de-noising and amplifying. Note that the collected ECG data will be stored locally in remember card of ECG module and can be transmitted to the cloud platform via WiFi network and TCP/IP network protocol. The ECG module also includes a Bluetooth deliver module to transmit the ECG signal to smartphone in real time.

For network layer, a Bluetooth receive module is used to acquire the ECGs from smartphone. Meanwhile, smartphone can access to cloud platform by 4G network and TCP/IP network, to upload data or download reports generated in cloud platform. In addition, a WiFi module can upload the stored long-term ECGs in ECG module to cloud platform at a preset frequency.

Cloud platform first serves as an cloud ECG database, providing structured data saving and management. More importantly, it implements artificial intelligence (AI) and cloud computing tasks for big ECG data processing, providing valuable disease prediction and diagnosis.

The application layer has the multiple interactions with the other layers. In general, it includes two function modules: one is real-time analysis and another one is post-processing. For users, the real-time analysis module receives the ECGs from the user-side and implements the real-time signal processing on the application program installed in smartphone (see Fig. 2), including the detections of QRS complex, P wave and T wave, as well as heart rate (HR), ST segment, *etc*. Then the analysis reports can be generated and can be uploaded to cloud platform as required. For doctors, the real-time analysis module can provide a real-time display of ECGs and individual user's reports via the Web server (see Fig. 3). The saved individual healthiness status is also provided to facilitate the doctors' in-depth diagnosis. The post-processing module mainly performs the complicated diagnosis and prediction

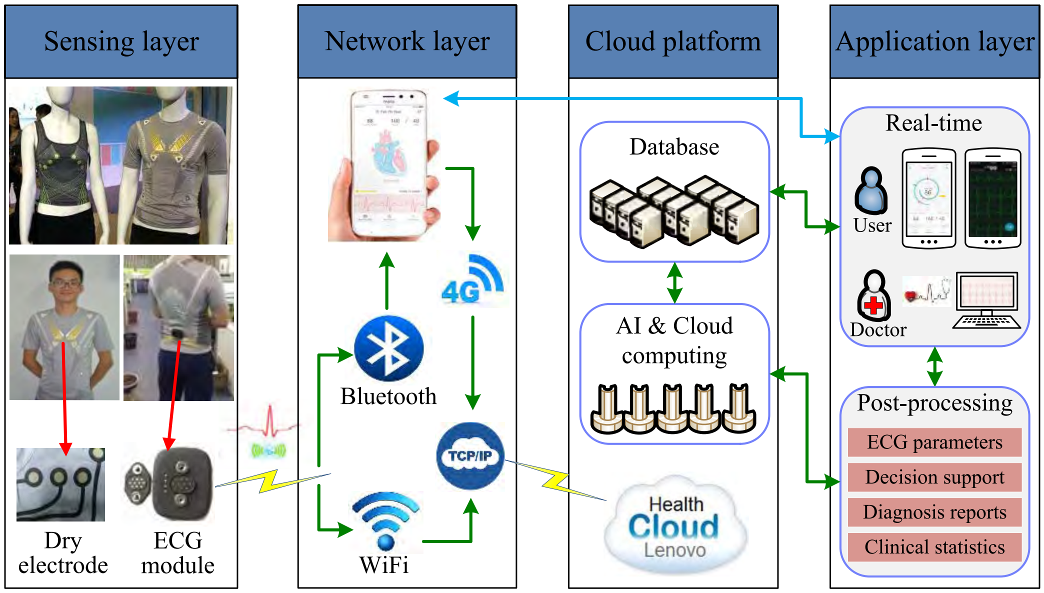

Fig. 1. Architecture of the developed Wearable 12-lead ECG SmartVest system.

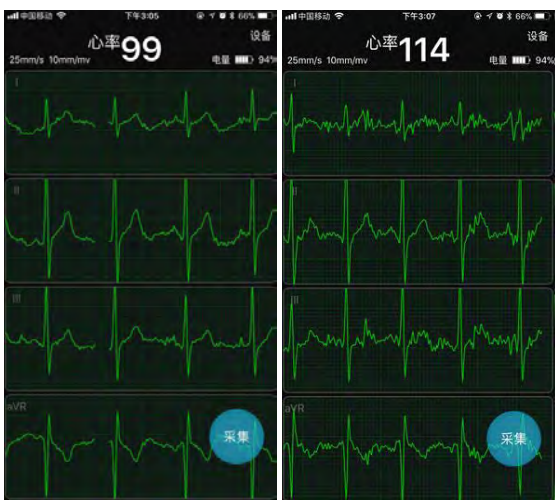

(a) (b)

Fig. 2. Application program on smartphone to facilitate the uses to observe the ECGs and real-time parameters, such as HR information. ECG waveforms from two recordings states are shown: (a) resting and (b) running states. It is clear that the recorded ECGs are clear even during the running state.

analysis for CVD risks, using the data mining, machine learning, and AI technologies, to provide comprehensive parameter results, decision support, systematical diagnosis report.

III. Signal Quality Assessment and Lightweight QRS Detection Algorithms

Accurate SQA and QRS detection for wearable ECGs is essential not only for the smartphone-side application but also for the application in cloud server, such as AI and cloud computation for big ECG data. Herein, we separately detail the mechanisms for SQA and lightweight QRS detection algorithms for the real-time and dynamic ECG monitoring application.

A. Signal Quality Assessment

1) Lead-Fall Detection: Lead-fall appears when the ECG amplitude keeps a constant for a preset time length. According to Hayn's study [35], ECG is detected as lead-fall signal if the portion of samples with constant amplitude is higher than 80%.

2) Signal Quality Indices: SQIs measures the signal quality or noise levels in ECGs. Typical SQIs were extensively studied in previous works [16], [36], [37]. SQIs used in this paper include the following.

a) bSQI: bSQI assesses the agreement level of two QRS detectors within a fixed time window. The hypothesis here is the presence of noises in ECG can lower the agreement level between two semi-independent QRS detectors. The independence of QRS detectors is important. The original bSQI proposed by Li *et al.* is based on two well documented open-source QRS detection algorithms: P&T algorithm based on digital filtering and integration [23] and *wqrs* algorithm based on a length transform after filtering [37]. For a *w*-second signal window, bSQI is defined as the ratio of beats detected synchronously by both algorithms to all the detected beats by either algorithm

$$\mathrm{bSQI} = \frac{N_{\mathrm{matched}}}{N_{\mathrm{P\&T}} + N_{wqrs} - N_{\mathrm{matched}}} \tag{1}$$

where N_{matched} is the number of beats that both algorithms agreed upon using a threshold of 150 ms, $N_{\mathrm{P\&T}}$ is the number of beats detected by P&T, and N_{wqrs} is the number of beats detected by *wqrs*. Therefore, bSQI ranges between 0 and 1.

b) tSQI: tSQI assesses the morphology consistency of any two ECG beats (with P&T QRS locations) within a fixed time window. The correlation matrix $C = [c_{ij}]$ is constructed, where c_{ij} is the correlation coefficient between the ith beat and the jth beat. tSQI is defined as

$$\mathrm{tSQI} = \frac{\sum_{i=1}^{M}\sum_{j=1}^{M} c_{ij}}{M^2} \tag{2}$$

where M is the beat number in a fixed time window.

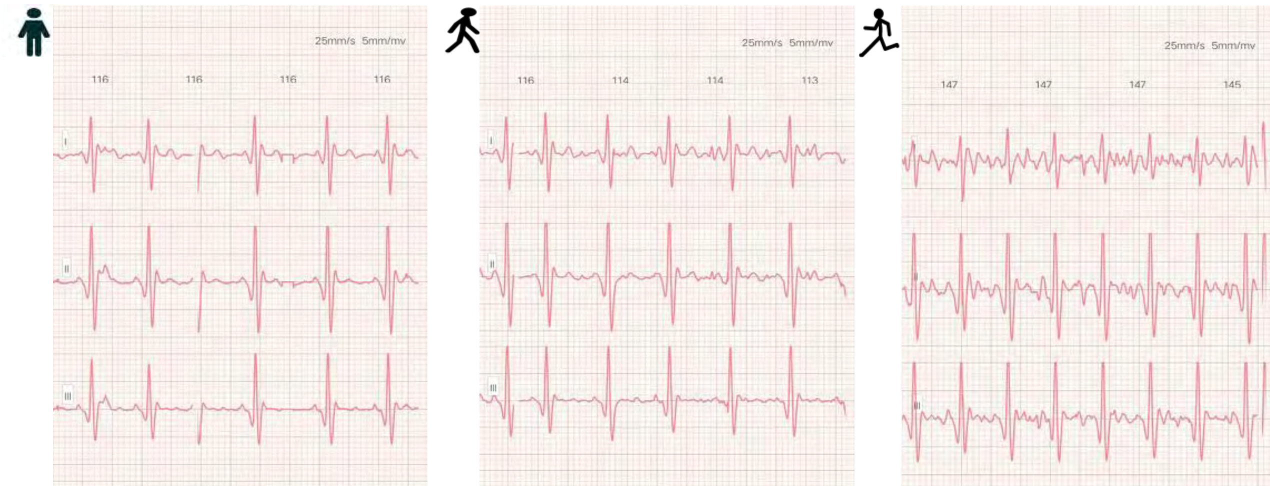

(a) (b) (c)

Fig. 3. Demonstrations of ECG waveforms for a real-time display via the Web server to facilitate the doctors' observations. ECGs are from three recording states: (a) resting, (b) walking, and (c) running. In each subfigure, the three limb lead ECGs, i.e., lead I, II, and III, are shown, with the calculated HR values for each heart beat.

c) iSQI: iSQI assesses the interval abnormal index for RR interval time series (with P&T QRS locations) with a fixed time window. RR intervals are sorted in ascending order and then the 15% percentile value RR_{15} and 85% percentile value RR_{85} are selected, and iSQI is defined as

$$\mathrm{iSQI} = \frac{RR_{15}}{RR_{85}}. \tag{3}$$

d) aSQI: aSQI assesses the high amplitude artifact in ECGs. In general, the signal amplitude in normal ECGs is 2.5–3.0 mV. Huge impulses ($\geq$5 mV) exist in situations of motion artifacts, or huge baseline wander. We count the times Tn that the amplitude changes are larger than 5 mV for a nonoverlap sliding window (0.2 s), and define aSQI as

$$\mathrm{aSQI} = \exp\left(-\left(\frac{Tn}{5}\right)^2\right). \tag{4}$$

e) pSQI: pSQI assesses the power spectrum distribution feature. ECG waveform usually has a frequency range of 0.05–125 Hz for clinical diagnosis and a frequency range of 0.05–45 Hz for clinical monitoring. High signal quality ECGs usually have a distinguishable QRS complex, which has a frequency range from several to a dozen of Hz [16], [37]. So, the ratio of power spectral density in the QRS energy band to that in the overall energy band provides a useful measure, thus pSQI is defined as

$$\mathrm{pSQI} = \frac{\int_{5\mathrm{Hz}}^{15\mathrm{Hz}} P(f)df}{\int_{5\mathrm{Hz}}^{45\mathrm{Hz}} P(f)df} \tag{5}$$

where $P(f)$ is the autoregressive (AR) model spectrum and the Burg algorithm is adopted for parameter estimation.

f) sSQI: sSQI is the third moment (skewness) of the ECG signal distribution [16], [37], and is defined as

$$\mathrm{sSQI} = \left|\frac{1}{N}\sum_{i=1}^{N}\left(\frac{(x_i-\mu)}{\sigma}\right)^3\right| \tag{6}$$

where x_i is the ECG signal with N sample points, μ is the signal mean, and σ is the standard deviation (SD), $|\cdot|$ means the absolute value.

g) kSQI: kSQI is the fourth moment (kurtosis) of the ECG signal distribution [16], [37], and is defined as

$$\mathrm{kSQI} = \frac{1}{N}\sum_{i=1}^{N}\left(\frac{(x_i-\mu)}{\sigma}\right)^4 \tag{7}$$

where all parameters have the same meanings with sSQI.

3) Nonlinear Features: The nonlinear features are expected to address the inherent nonlinear characteristic in ECGs. They have been applied in the SQA in previous studies [38], [39]. Herein, we include the following nonlinear features as SQIs, most of which are new developed.

a) Sample entropy: Entropy refers to the degree of regularity or irregularity of a signal [40], [41]. Sample entropy (SampEn) is widely used one. Repeated patterns imply increased regularity in the signal and lead to low SampEn values. By contrast, random Gaussian noises can output large entropy values. SampEn is especially sensitive to Gaussian noises in ECGs [39].

b) Fuzzy measure entropy: Decision rule for vector similarity in SampEn is based on Heaviside function, and its rigid boundary effect may induce to the poor stability, and even failure to define the entropy if no vector-matching could be found [42], [43]. As an improved version, Fuzzy measure entropy (FuzzyMEn) uses a fuzzy membership function to replace the Heaviside function, and combines both local and global similarities for entropy calculation, giving a better discrimination for time series [44].

c) Lempel-Ziv complexity: Lempel-Ziv (LZ) is a complexity measure, and has been applied as an ECG signal quality index [45]. The classical LZ complexity consists of two steps. First, an original time series is transformed into a new binary symbolic sequence, and then LZ value is calculated by counting the new patterns in the binary sequence.

d) Encoding LZ complexity: Encoding LZ (ELZ) can not only distinguish chaotic and random characteristics in ECGs but also can indicate the noise level, especially for ECGs corrupted by high frequency noise [46]. For ELZ calculation, the original signal is transformed into an 8-state symbolic (3-bit binary) sequence by an encoding approach.

4) Features Normalization: Since the nonlinear features have much higher computation complexity, in this paper, we only consider the seven SQIs for real-time SQA used in smartphone-side. These SQIs form the real-time signal quality vector as

$$\mathrm{SQI}_{\mathrm{real-time}} = \left[\mathrm{bSQI}, \mathrm{tSQI}, \mathrm{iSQI}, \mathrm{aSQI}, \mathrm{pSQI}, \mathrm{sSQI}, \mathrm{kSQI}\right]. \tag{8}$$

For SQA used in cloud server, the signal quality vector is added with the nonlinear features as

$$\mathrm{SQI}_{\mathrm{cloud}} = \left[\mathrm{bSQI}, \mathrm{tSQI}, \mathrm{iSQI}, \mathrm{aSQI}, \mathrm{pSQI}, \mathrm{sSQI}, \mathrm{kSQI}, \mathrm{SampEn}, \mathrm{FuzzyMEn}, \mathrm{LZ}, \mathrm{ELZ}\right]. \tag{9}$$

For each of the feature vectors X, we normalize them by subtracting the median value X_{median} (less prone to outliers than the mean) and dividing by the SD σ_X as

$$X = \frac{X - X_{\mathrm{median}}}{\sigma_X}. \tag{10}$$

The mean and SD from the training set were used for both the training and test set when normalizing.

B. Lightweight QRS Detection Algorithm

For long-term wearable ECG monitoring, noises are wide-sourced, and sometimes are unexpected due to the unexpected human activities. In SQA step, we weight more priority to reserve the relatively noisy ECGs rather than to exclude them, i.e., we want to make full use of the recorded ECGs and assess them as clean/useful for the following signal analysis. Thus, the QRS detection step is challenging. The main hurdle we have to overcome is to ensure high detection accuracy in the selected relatively noisy ECGs. Meanwhile, the developed algorithm should be lightweight and has small calculation burden, to facilitate the real-time analysis on smartphone-side. Dynamic ECG detection is usually challenged by motion artifacts due to the unexpected motion intensity and motion state, and the noises due to the change of relative displacement between electrode and skin. These noises have typical characteristics as large baseline wander and transient high amplitude impulse. Thus we specifically consider the corresponding strategies to solve out this challenges and detail it as below.

First, in order to deal with the large baseline wander, we consider a correction algorithm which involves a combination of a high order linear-phase filter and a sliding window averaging to remove the influence of large baseline wander.

Second, in order to deal with the transient high amplitude impulse, we use an amplitude calibration technique with the combination of signal filtering to weaken noise amplitude and enhance the amplitude of QRS complex.

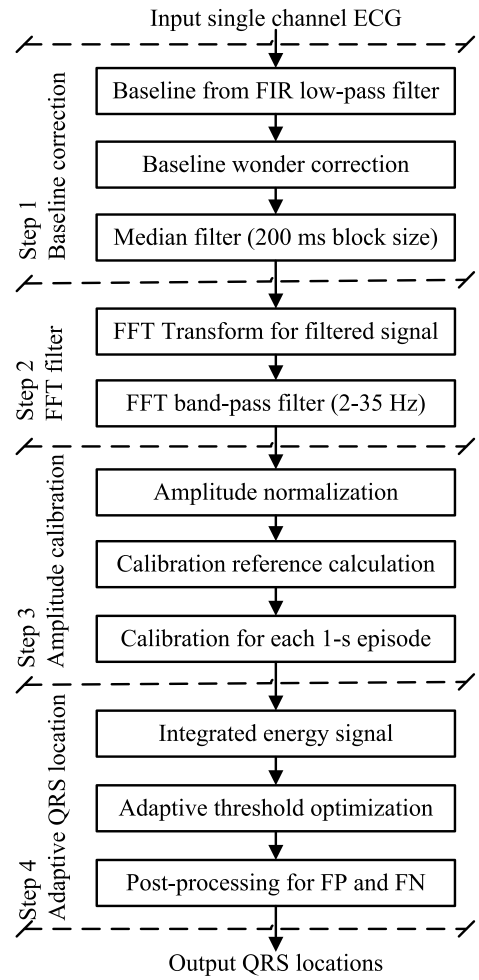

Fig. 4. Flowchart of the proposed lightweight QRS detector.

Third, finding an optimal threshold for QRS detector is another challenge. The high amplitude T waves and impulses can disturb the identification of QRS complexes. In addition, the ECG waveforms vary not only for signals from different subjects but also for those collected from the same subject due to the difference motion states. Therefore, an adaptive mechanism for threshold updating needs.

Last, all approaches should consider the calculation burden on the smartphone-side for real-time signal processing and feedback, and they should be computationally efficient.

So the proposed QRS detection algorithm consists of four key steps including baseline correction, fast Fourier transformation (FFT) band-pass filter, amplitude calibration, and adaptive QRS location. The algorithm flowchart is illustrated in Fig. 4. Each step is detailed as follows.

Step 1 (Baseline Correction): Baseline wander below 7.5 Hz was extracted from the raw ECG using an order 200 finite impulse response low-pass filter, which was a common Hamming-window based, linear-phase and all-zero filter. Then the filtered ECG was obtained by removing the baseline wander from the raw ECG, and was refiltered by an order 10 median filter with 200 ms block size.

Step 2 (FFT Band-Pass Filter): In this step, baseline removed signal was filtered by an FFT band-pass filter, with the frequency range of 2–35 Hz. Using FFT band-pass filter aimed to enhance the implement efficiency of QRS detector embedded in smartphone.

Step 3 (Amplitude Calibration): The filtered signal after Step 2 was then inputted an amplitude calibration module. First, the signal was normalized and the negative values were depressed. Then the module sliced the signal into 1-s time length ECG episodes, and calculated the signal amplitude in each episode, and then sorted these amplitude values from all 1-s ECG episodes in a 10-s window size. The median amplitude value was identified as the calibration reference for each 1-s ECG episode, and all 1-s ECG episodes were calibrated to fit this calibration reference.

Step 4 (Adaptive QRS Location): The filtered signal after amplitude calibration was transferred into an integrated energy signal. An adaptive amplitude threshold was employed to detect QRS peak candidates in the integrated energy signal. This adaptive amplitude threshold was initially set as $A_p = 0.6$ times of the calibration reference for each 1-s ECG episode in the Step 3, and then automatically updated based on the number of the detected QRS peaks with the following criteria:

$$A_p = \begin{cases} 0.5 & \text{number of } QRS < 8 \\ 0.7 & \text{number of } QRS > 14. \end{cases} \tag{11}$$

Then, an optimization step was performed by rechecking the adjacent RR intervals from all detected peaks. The RR interval less than 360 ms was rechecked to see whether it was a false positive QRS detection and the RR interval larger than 1.5 s was rechecked to see whether a false negative QRS. We compared the RR interval less than 360 ms with the mean value and confirmed the false positive when the mean value is 1.8 times larger than the checked RR interval. Similarly, we compared the RR intervals larger than 1.5 s with the mean value, and confirmed the false negative when the mean value is 0.6 times less than the checked RR interval. Finally, a 200 ms refractory blanking technology was used to optimize the detected QRS locations. The rechecking and optimization were performed on the 10-s signal window.

IV. Experiment Designs

A. Data Recording and Labeling

Long-term ECG data during daily activities were collected using the developed SmartVest system, with a sample rate of 500 Hz and a 12-bit resolution. Signal recording lasted from March 2017 to October 2017, generating a total of 317 recordings with varied time length.

Extremely noisy ECGs are the main challenge for real-time and dynamic ECG processing. To deal with this, first, we visually inspected the recorded ECGs and manually selected about 1000 of 10-s single-channel ECG segments with different signal quality situations (from slightly noisy to extremely noisy). As comparison, a part of clean 10-s single-channel ECG segments were also selected. The single-channel ECG segments can be from any of the 12 leads of I, II, III, aVR, aVL, aVF, V1, V2, V3, V4, V5, and V6. Then, three independent annotators were asked to label the selected 10-s single-channel ECG segments into five different signal quality levels: A to E. The interpretation of signal quality labeling criteria was summarized in Table II. If two or more annotators agreed with the quality labeling, the quality annotation on this 10-s segment was confirmed. This paper was performed using a MATLAB (MathWorks, Natick, MA, USA) graphical user-interface (GUI) interface. Annotated 10-s ECG single-channel segments were summarized in Table I. Typical examples in each signal quality level were shown in Fig. 5. ECG segments from Level E type were too noisy and should be excluded. We identified all ECG segments in Levels A to D as acceptable whereas those from Level E as “unacceptable,” for our wearable ECG monitoring.

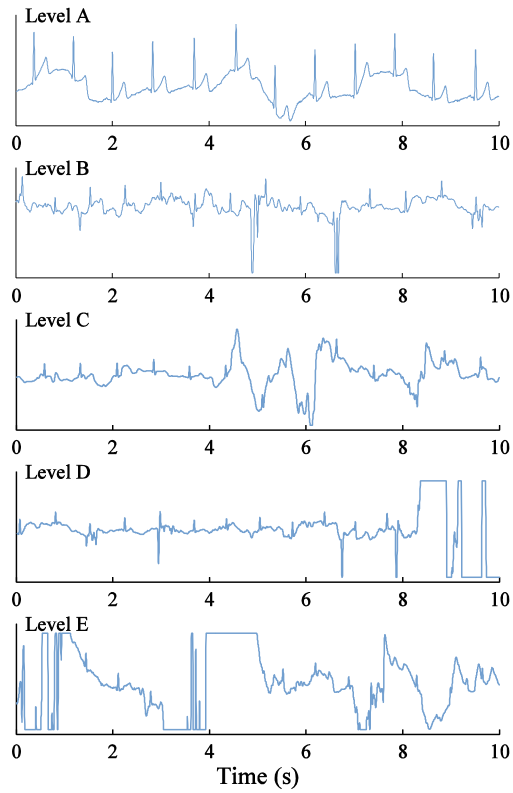

Fig. 5. Typical 10-s single-channel ECG segments from each signal quality level. ECG segments from Levels A-E have the decreased signal quality.

B. Online Open ECG Data

1) PhysioNet/CinC Challenge 2014 Database: This database included 200 ECG recordings from the 2014 PhysioNet/CinC Challenge, which were separated into two subdatabases: 1) 100 recordings with high signal quality as the training set (denoted as Test set A) and 2) another 100 recordings with low signal quality as the augmented training set (denoted as Test set B). The former was sampled at 250 Hz and the latter was sampled at 360 Hz. Each recording had a time length of 10 min. Reference QRS locations were provided [47].

1) Telehealth ECG Database: This database (denoted as Test set C) included 250 telehealth ECGs (only lead-I ECGs, sample rate as 500 Hz, time length 30 s) recorded by

TABLE I
SUMMARY OF THE SELECTED 10-S SINGLE-CHANNEL ECG SEGMENTS FOR EACH SIGNAL QUALITY LEVEL

Level	# 10-s ECGs	Interpretation of signal quality labeling
Level A	200	ECGs have clear QRS complex and T wave. Baseline wander does not influence the identification for QRS.
Level B	197	Transient high amplitude impulse exists, but no more than three episodes. The majority of QRS complexes can be visually clearly identified.
Level C	181	Both large baseline wander and transient high amplitude impulse exist. It is challenging to visually clearly identify the QRS complexes in a 2-3 s time window.
Level D	175	More serious large baseline wander and transient high amplitude impulse exist than Level C. At least a 2-3 s signal episode are totally noises, making the identification for QRS complexes in this episode impossible. However, at least 4-5 s signal episode has visually identifiable QRS complexes.
Level E	196	Signal quality is worse than Level D. More than half of the ECG segment are pure noises. Large baseline wander, transient high amplitude impulse and signal saturation occupy the majority. Continuous visually identifiable QRS complexes are less than four.

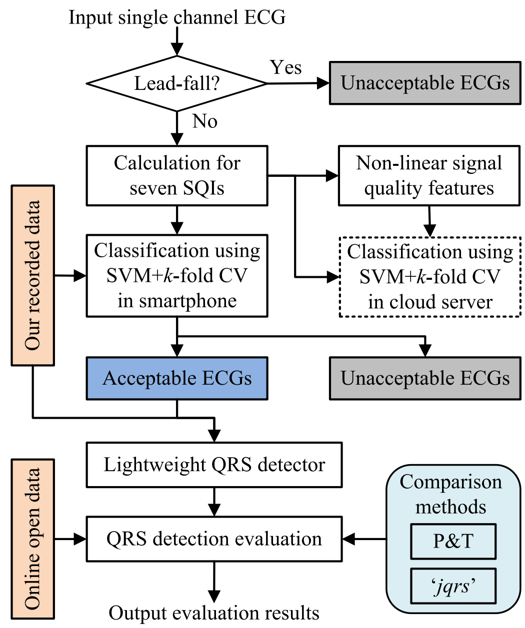

Fig. 6. Evaluation procedure for the SQA and lightweight QRS detection algorithms.

the TeleMedCare Health Monitor (TeleMedCare Pty., Ltd., Sydney, Australia). Signals were collected using dry metal electrodes and were recorded in an unsupervised environment. Reference QRS locations were also provided [33].

C. Evaluation Methods

The evaluation procedure was presented in Fig. 6. Data recorded by our SmartVest system were used for training the SQA algorithm. First, ECG segment was identified if it was a lead-fall signal. Then seven SQIs were calculated to train a signal quality classification model for smartphone application. In addition, for cloud server application, where the computation cost was not limited, the nonlinear signal quality features were also calculated.

We used the open-source libsvm software package to train and learn an SVM-based classification model [48]. Tenfold cross-validation method was used to enhance the generalization ability of the trained model. The default parameters for SVM were: radial basis function as the kernel function, gamma parameter $\gamma = 0.1$ in kernel function, cost parameter $C = 1$. Thus the ECG segments could be identified as acceptable (levels A–D) or unacceptable (level E).

Then the acceptable segments were used to train the lightweight QRS detector for optimizing its thresholds and parameters. ECGs from online open databases were used for test, which includes 72 415 QRS complexes for Test Set A, 78 681 for Test Set B, and 6708 for Test Set C. The reference QRS labels were used as the benchmarks for algorithm evaluation. Two existing QRS detectors of P&T [23] and *jqrs* [32] were used as comparison methods. We also performed the QRS detectors on each of 10-s ECG episode.

Let denotes the reference QRS positions. For the *i*th position x_i, we counted the numbers of detected QRS within time regions: $[x_i - \delta x_i + \delta]$ and $(x_i + \delta x_{i+1} - \delta)$. Parameter δ was a tolerate for determining the true positive (TP), false positive (FP) and false negative (FN) QRS detections and was set as 50, 100, and 150 ms, respectively, in this paper. Finally, the evaluation metrics of sensitivity (Se), positive predictivity (P_+), and F_1-score as the geometric average of the former two metrics were calculated as

$$\mathrm{Se} = \frac{\mathrm{TP}}{\mathrm{TP} + \mathrm{FN}} \times 100\% \tag{12}$$

$$P_+ = \frac{\mathrm{TP}}{\mathrm{TP} + \mathrm{FP}} \times 100\% \tag{13}$$

$$F_1 = \frac{2 \times \mathrm{Se} \times P_+}{\mathrm{Se} + P_+} \times 100\%. \tag{14}$$

In addition, the computation cost for the mobile application is important. We compared the time costs between the proposed method and the traditional P&T and *jqrs* algorithms by analyzing the 10-s ECG segments on the used online open databases. The evaluation was implemented in a MATLAB 2014a environment (The MathWorks Inc., Natick, MA, USA) on an Intel i5 CPU 3.30 GHz.

V. RESULTS

A. Signal Quality Assessment Results

The overall signal quality classification results for the 10-s ECG segments were summarized in Table II. SVM-based signal quality classification model achieved 100% correct classifications for ECG segments in Levels A, B, and C. Correct classifications for the majority in Levels D (90.9%) and E (96.4%) were also achieved. The SVM-based model can achieve an average accuracy of 97.9% and 96.4% for acceptable and unacceptable ECG segments, respectively, verifying the model efficiency to select good or exclude poor quality ECG segments in the real wearable ECG monitoring.

TABLE II
PERFORMANCE OF THE SVM-BASED SIGNAL QUALITY CLASSIFICATION MODEL USING A TENFOLD CROSS VALIDATION

Level	Annotation	# recording	TC	FC	Acc (%)
Level A	acceptable	200	200	0	100
Level B	acceptable	197	197	0	100
Level C	acceptable	181	181	0	100
Level D	acceptable	175	159	16	90.9
Levels A-D	acceptable	753	737	16	97.9
Level E	unacceptable	197	190	7	96.4

Note: TC, total number of the true classification from 10-fold cross validation; FC, total number of the false classification from 10-fold cross validation; $Acc = \frac{TC}{TC+FC} \times 100\%$, classifcation accuracy.

B. QRS Detection Results

Fig. 7 shows an example of the lightweight QRS detector, with the comparison of P&T and *jqrs*. The new QRS detector output less false positive and false negative detections than the two comparable methods. Table III shows their performances on the test data under three types of tolerate δ: 50, 100, and 150 ms, respectively. All three QRS detectors achieved high detection accuracy (all $F_1 \geq 99.5\%$) for Test set A (a relative high quality database) but had relatively low detection accuracy (all $F_1 < 91\%$) for Test sets B and C (poor quality databases). F_1-values showed the three QRS detectors had no significant differences for Test set A, but had obvious differences for Test sets B and C. The new QRS detector achieved the highest F_1 results for Test sets B and C, at each of three tolerate types.

Specifically, when $\delta = 50$ ms, P&T reported F_1-values of 79.02% and 72.69% for Test sets B and C, *jqrs* reported F_1-values of 78.38% and 73.99%, whereas the new one achieved F_1-values of 80.09% and 76.60%, with about 1–2% improvement for Test set B and 3–4% improvement for Test set C. From Table III, it can be noted that P&T generated more FP detections than *jqrs*, while the latter generated more FN detections than the former. However, the new method kept the advantages for both comparable methods, and achieved a good balance between FP and FN detections.

With the increase of tolerate δ, detection accuracy increased for all three QRS detectors. When δ increased from 50 ms to 150 ms, F_1-values of P&T increased from 79.02% to 86.28% and then to 88.45% for Test set B, and increased from 72.69% to 76.12% and then to 76.39% for Test set C. F_1-values of *jqrs* increased from 78.38% to 85.20% and then to 86.59% for Test set B, and increased from 73.99% to 75.37% and then to 75.60% for Test set C. For the new detector, F_1-values increased from 80.09% to 87.66% and then to 90.31% for Test set B, and increased from 76.60% to 78.17% and then to 78.41% for Test set C. Similar F_1 result trends appeared for the three QRS detectors with the change of tolerate δ.

For computation efficiency evaluation, P&T and *jqrs* reported similar mean time costs (3.2 ms versus 3.1 ms) on 10-s ECG segments. Meanwhile, *jqrs* had a much larger SD (0.4 ms versus 0.9 ms) than P&T. The proposed lightweight algorithm had the highest computation efficiency (Mean: 2.3 ms, SD: 0.7 ms), generating 28% and 26% time cost decreases compared with the P&T and *jqrs* methods, respectively.

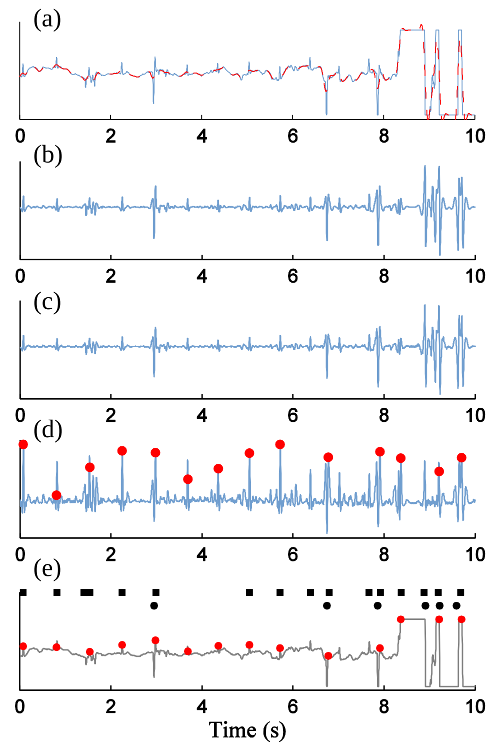

Fig. 7. Example for demonstrating the lightweight QRS detector. (a) Raw 10-s ECG segment with the baseline wander (red dashed line). (b) ECG after baseline wander correction. (c) ECG after FFT band-pass filter. (d) ECG after amplitude calibration (detected QRS complexes as solid circles). (e) QRS complexes (red solid circles) were identified in raw ECG. As a comparison, detected QRS by P&T (black solid squares) and *jqrs* (black solid circles) were also shown.

VI. DISCUSSION

The requirement for real-time long-term ECG monitoring is growing. A traditional ECG Holter is often inconvenient to carry because it attaches many electrodes to the chest. Wearable ECG devices have been developed in the past several years [4], [7], [10], [49]. For better understanding the need of remote and continuous ECG monitoring, as well as why the wearable and IoT technologies can help, we briefly summarized the developments of ECG devices as four generations, and demonstrated the typical devices in Fig. 8, with the summary of their characteristics in Table IV. The first-generation device [Fig. 8(a)] is the traditional ECG scan device that widely used in clinic, which collects the patients' 12-lead ECGs for dozens of seconds in a rest and quiet environment. ECGs recorded in this way have high signal quality, providing the doctor opportunity for manually identifying tiny changes in waveforms. However, since many pathological situations are silent during the resting recording due to the asymptomatic or intermittent in CVDs, the first-generation device can miss the useful ECG episode. Holter [Fig. 8(b)] is the second-generation ECG device, which can record up to 24 h multichannel ECGs. The long-term ECGs are essential for detecting the asymptomatic or intermittent CVD situations.

TABLE III
PERFORMANCES OF THE THREE QRS DETECTORS ON THE ONLINE OPEN DATABASES AT THREE TYPES OF TOLERATE: 50, 100, AND 150 ms, RESPECTIVELY

Tolerate δ	Database	Method	Total beat	TP	FP	FN	Se (%)	P_+(%)	F_1 (%)
50 ms	Test set A	P&T	72,415	71,987	281	428	99.41	99.61	99.51
		jqrs	72,415	72,041	67	374	99.48	99.91	99.69
		Proposed	72,415	71,946	151	469	99.35	99.79	99.57
	Test set B	P&T	78,618	64,916	20,764	13,702	82.57	75.77	79.02
		jqrs	78,618	61,078	16,156	17,540	77.69	79.08	78.38
		Proposed	78,618	64,471	17,908	14,147	82.01	78.26	80.09
	Test set C	P&T	6,708	5,952	3,716	756	88.73	61.56	72.69
		jqrs	6,708	4,878	1,599	1,830	72.72	75.31	73.99
		Proposed	6,708	6,159	3,213	549	91.82	65.72	76.60
100 ms	Test set A	P&T	72,415	72,106	162	309	99.57	99.78	99.67
		jqrs	72,415	72,063	45	352	99.51	99.94	99.73
		Proposed	72,415	71,989	108	426	99.41	99.85	99.63
	Test set B	P&T	78,618	70,878	14,802	7,740	90.15	82.72	86.28
		jqrs	78,618	66,396	10,838	12,222	84.45	85.97	85.20
		Proposed	78,618	70,567	11,812	8,051	89.76	85.66	87.66
	Test set C	P&T	6,708	6,233	3,436	475	92.92	64.46	76.12
		jqrs	6,708	4,969	1,508	1,739	74.08	76.72	75.37
		Proposed	6,708	6,285	3,087	423	93.69	67.06	78.17
150 ms	Test set A	P&T	72,415	72,121	152	294	99.59	99.79	99.69
		jqrs	72,415	72,084	25	331	99.54	99.97	99.75
		Proposed	72,415	72,027	73	388	99.46	99.90	99.68
	Test set B	P&T	78,618	72,685	13,046	5,933	92.45	84.78	88.45
		jqrs	78,618	67,480	9,770	11,138	85.83	87.35	86.59
		Proposed	78,618	72,711	9,698	5,907	92.49	88.23	90.31
	Test set C	P&T	6,708	6,257	3,416	451	93.28	64.69	76.39
		jqrs	6,708	4,984	1,494	1,724	74.30	76.94	75.60
		Proposed	6,708	6,305	3,069	403	93.99	67.26	78.41

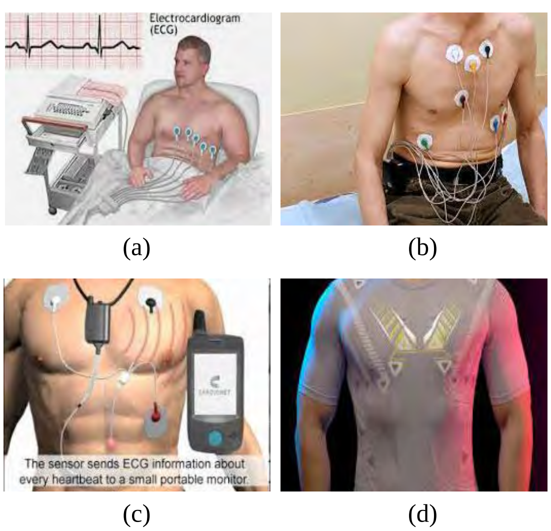

Fig. 8. Demonstrations of the four generations of ECG devices.

TABLE IV
SUMMARY OF THE CHARACTERISTICS OF THE FOUR GENERATIONS OF ECG DEVICES

Characteristics	ECG devices			
	First-generation	Second-generation	Third-generation	Fourth-generation
Recording length	Short-term (dozens of seconds)	Long-term (up to 24 hours)	Long-term (up to 24 hours or more)	Long-term (up to 24 hours or more)
Recording state	Only rest	Rest and dynamic	Rest and dynamic	Rest and dynamic
Signal quality	Clean	Noisy	Noisy	Noisy
Signal real-time analysis	No	No	Yes	Yes
ECG electrode	Ag/AgCl wet electrode	Ag/AgCl wet electrode	Ag/AgCl wet electrode	Textile dry electrode
Possible skin allergy?	Yes	Yes	Yes	No
Wearable?	No	No	No	Yes
Comfort	Low	Low	Low	High

However, signal processing and diagnosis analysis in Holter is hysteretic. This type device only records the 24-h ECGs in a memory card without any real-time analysis. Thus, it is blind for real-time feedback for disease risk. In addition, the post-processing for 24-h data brings a heavy burden for the backend server. Thus, the third-generation ECG device is developed, which is a Holter-like device but adds a wireless module to transmit the ECG waveforms to a portable smartphone or similar device. The smartphone is required to take real-time and intelligent signal analysis task, to identify normal, abnormal, or pathological situations. Whatever the second-generation Holter or the third-generation Holter-like device, it uses Ag/AgCl wet electrodes, and the Ag/AgCl electrode requires conductive gel to work efficiently. However, conductive gel can dehydrate in a few hours, resulting in the degradation of signal quality in the long-term monitoring [6]. Meanwhile, conductive gel can cause irritation and allergy on the skin. It can hardly meet the comfort requirement for long-term monitoring [5], [10]. Thus, the wearable smart ECG garment is developed as the fourth-generation device, which uses the textile dry electrodes to improve the comfort in signal recording. Wearable smart garment is emerging as a promising technology for the miniaturization of devices for vital signs monitoring recently [10], [12], [50]. Wearable smart ECG garment combines the technologies of textile sensor, ergonomic design, big data, cloud computing, machine learning, and can be served as an ideal IoT monitoring terminal. Fig. 8(d) shows an example of the fourth-generation device, i.e., the wearable 12-lead ECG SmartVest system, which is jointly developed by our Lab in Southeast University and Lenovo Research Institute. Other typical wearable ECG devices include: Vital-Jacket developed by the University of Aveiro, Portugal [51], wearable context-aware ECG monitoring system with built-in Kinematic sensors [52], wearable ECG unit [53], etc.

The advantages of the new developed IoT-based SmartVest system are: 1) the ergonomic design was used for the manufacture to unsure the comfort of the cloth; 2) the dry electrode was optimized from the comparison among several different textile materials, which was verified in our previous study [12]; 3) we constructed a could platform for big-data ECG monitoring and processing; and 4) last but not least, we focused on the efficient SQA method and lightweight QRS detection for single-channel ECG processing on the developed system, and verified the performances.

For IoT-driven wearable application, the tradeoff between keeping a low quality recording or discarding a good quality recording is always a key issue. This paper proposes a combination method of multiple SQIs and SVM-based machine learning for automatically classifying the signal quality of acquired ECGs under resting, ambulatory and physical activity environments. The results demonstrate that the proposed method can efficiently deal with the tradeoff between accepting good (97.9%) and rejecting poor (96.4%) quality signals and can efficiently reserve ECG segments with diagnosis value from the severely distorted signals, ensuring that only a low percentage of recorded ECGs are discarded, thereby reducing the unnecessary recollection of the recordings and enhancing resource utilization efficiency of IoT-enabled devices. This is critical for the wearable monitoring systems.

Meanwhile, we developed a new lightweight QRS detector for robustly identifying QRS complex from the noisy ECGs, and achieved high detection performances with low computation cost. The new QRS detector had a F_1 score ($\geq$ 99.5%) as high as the two existing methods (P&T and *jqrs*) for clean ECGs (Test set A) while achieved a significantly higher F_1-value for noisy ECGs (Test set B). Evaluation results on the real collected telehealth environment (Test set C) further verified its high sensitivity (Se $\geq$ 90%) by generating much less FN QRS detections, which is important for real-time ECG parameters, such as HR values and HR changes. In addition, the proposed lightweight QRS detector also showed a significant computation efficiency, with 28% and 26% time cost decreases compared with the P&T and *jqrs* algorithms, respectively.

Potential limitations should be discussed. First, the developed algorithms in this paper focused on the daily activities monitoring. The monitored population are commonly healthy subjects without serious CVD situations. The challenge here is mainly the robust QRS detection under extremely noisy environment. The current work did not include the test on the challenging pathological conditions such as ventricular fibrillation or ventricular tachycardia detection. Meanwhile, it also was not designed to deal with the pacemaker situation, which cannot be processed by a 2–35 Hz band-pass filter. Second, the algorithms developed in current work is based on single-channel ECG analysis, without considering that the inter channel agreement metrics can benefit for the SQA or the information fusion approach can benefit the QRS locations. We identify these two points as our future works. Finally, although we have achieved high classification accuracy for acceptable and unacceptable 10-s ECG segments, the classification criteria for the five signal quality levels can be further refined.

VII. Conclusion

In this paper, we present a novel IoT-based Wearable 12-lead ECG SmartVest system for cardiovascular health monitoring applications. The IoT-driven system can collect multichannel ECGs using textile dry ECG sensors, implement the automatic real-time and accurate signal analysis in smartphone-side, and then employ wireless connectivity to transmit gathered ECGs and analyzed results directly to the cloud server and the doctors for further clinical review. In this IoT-monitoring mode, the ECG SmartVest system saves the medical resources in terms of the medical cost and the time of physicians. The results presented here indicate that is possible to accurately classify the signal quality and detect the QRS complexes for wearable ECGs in real time, and thereby provide a real-time accurate and time cost efficient feedback (such as signal quality, heart rate, disease risk, *etc.*) for the developed Wearable ECG SmartVest system. Thus, the IoT-based Wearable 12-lead ECG SmartVest system is suitable to be applied to the massive CVD-prone population and holds promising application future.

References

[1] GBD 2015 Mortality and Causes of Death Collaborators, "Global, regional, and national life expectancy, all-cause mortality, and cause-specific mortality for 249 causes of death, 1980-2015: A systematic analysis for the Global Burden of Disease Study 2015," *Lancet*, vol. 388, no. 10053, pp. 1459–1544, 2016.

[2] H. C. McGill, C. A. McMahan, and S. S. Gidding, "Preventing heart disease in the 21st century: Implications of the pathobiological determinants of atherosclerosis in youth (PDAY) study," *Circulation*, vol. 117, no. 9, pp. 1216–1227, 2008.

[3] D. He and S. Zeadally, "An analysis of RFID authentication schemes for Internet of Things in healthcare environment using elliptic curve cryptography," *IEEE Internet Things J.*, vol. 2, no. 1, pp. 72–83, Feb. 2015.

[4] L. Catarinucci *et al.*, "An IoT-aware architecture for smart healthcare systems," *IEEE Internet Things J.*, vol. 2, no. 6, pp. 515–526, Dec. 2015.

[5] Y. Zhang, L. Sun, H. Song, and X. Cao, "Ubiquitous WSN for healthcare: Recent advances and future prospects," *IEEE Internet Things J.*, vol. 1, no. 4, pp. 311–318, Aug. 2014.

[6] J. Yoo, L. Yan, S. Lee, H. Kim, and H.-J. Yoo, "A wearable ECG acquisition system with compact planar-fashionable circuit board-based shirt," *IEEE Trans. Inf. Technol. Biomed.*, vol. 13, no. 6, pp. 897–902, Nov. 2009.

[7] U. Satija, B. Ramkumar, and M. S. Manikandan, "Real-time signal quality-aware ECG telemetry system for IoT-based health care monitoring," *IEEE Internet Things J.*, vol. 4, no. 3, pp. 815–823, Jun. 2017.

[8] Y. L. Zhang *et al.*, "Unobtrusive sensing and wearable devices for health informatics," *IEEE Trans. Biomed. Eng.*, vol. 61, no. 5, pp. 1538–1554, May 2014.

[9] S. A. Siddiqui, Y. Zhang, Z. Feng, and A. Kos, "A pulse rate estimation algorithm using PPG and smartphone camera," *J. Med. Syst.*, vol. 40, no. 5, p. 126, 2016.

[10] J. R. Windmiller and J. Wang, "Wearable electrochemical sensors and biosensors: A review," *Electroanalysis*, vol. 25, no. 1, pp. 29–46, 2013.

[11] M. T. I. Huque, K. S. Munasinghe, and A. Jamalipour, "Body node coordinator placement algorithms for wireless body area networks," *IEEE Internet Things J.*, vol. 2, no. 1, pp. 94–102, Feb. 2015.

[12] Z. P. Cai, K. Luo, C. Y. Liu, and J. Q. Li, "Design of a smart ECG garment based on conductive textile electrode and flexible printed circuit board," *Technol. Health Care*, vol. 25, no. 4, pp. 815–821, 2017.

[13] S. Amendola, R. Lodato, S. Manzari, C. Occhiuzzi, and G. Marrocco, "RFID technology for IoT-based personal healthcare in smart spaces," *IEEE Internet Things J.*, vol. 1, no. 2, pp. 144–152, Apr. 2014.

[14] S. Izumi *et al.*, "A wearable healthcare system with a 13.7 μA noise tolerant ECG processor," *IEEE Trans. Biomed. Circuits Syst.*, vol. 9, no. 5, pp. 733–742, Oct. 2015.

[15] Y.-T. Zhang, C.-Y. Liu, S.-S. Wei, C.-Z. Wei, and F.-F. Liu, "ECG quality assessment based on a kernel support vector machine and genetic algorithm with a feature matrix," *J. Zhejiang Univ. Sci. C*, vol. 15, no. 7, pp. 564–573, 2014.

[16] G. D. Clifford, J. Behar, Q. Li, and I. Rezek, "Signal quality indices and data fusion for determining clinical acceptability of electrocardiograms," *Physiol. Meas.*, vol. 33, no. 9, pp. 1419–1433, 2012.

[17] I. Silva, G. B. Moody, and L. Celi, "Improving the quality of ECGs collected using mobile phones: The PhysioNet/computing in cardiology challenge 2011," in *Proc. Comput. Cardiol.*, Hangzhou, China, 2011, pp. 273–276.

[18] I. Jekova, V. Krasteva, I. Christov, and R. Abächerli, "Threshold-based system for noise detection in multilead ECG recordings," *Physiol. Meas.*, vol. 33, no. 9, pp. 1463–1477, 2012.

[19] C. Y. Liu, P. Li, L. N. Zhao, F. F. Liu, and R. X. Wang, "Real-time signal quality assessment for ECGs collected using mobile phones," in *Proc. Comput. Cardiol.*, Hangzhou, China, 2011, pp. 357–360.

[20] S. Zaunseder, R. Huhle, and H. Malberg, "CinC challenge—Assessing the usability of ECG by ensemble decision trees," in *Proc. Comput. Cardiol.*, Hangzhou, China, 2011, pp. 277–280.

[21] Y. Chen and H. Yang, "Self-organized neural network for the quality control of 12-lead ECG signals," *Physiol. Meas.*, vol. 33, no. 9, pp. 1399–1418, 2012.

[22] H. Xia, G. A. Garcia, J. Bains, D. C. Wortham, and X. Zhao, "Matrix of regularity for improving the quality of ECGs," *Physiol. Meas.*, vol. 33, no. 9, pp. 1535–1548, 2012.

[23] J. Pan and W. J. Tompkins, "A real-time QRS detection algorithm," *IEEE Trans. Biomed. Eng.*, vol. BME-32, no. 3, pp. 230–236, Mar. 1985.

[24] P. S. Hamilton and W. J. Tompkins, "Quantitative investigation of QRS detection rules using the MIT/BIH arrhythmia database," *IEEE Trans. Biomed. Eng.*, vol. BME-33, no. 12, pp. 1157–1165, Dec. 1986.

[25] F. F. Liu *et al.*, "The accuracy on the common Pan-Tompkins based QRS detection methods through low-quality electrocardiogram database," *J. Med. Imag. Health Inform.*, vol. 7, no. 5, pp. 1039–1043, 2017.

[26] J. Giera *et al.*, "RS slope detection algorithm for extraction of heart rate from noisy, multimodal recordings," *Physiol. Meas.*, vol. 36, no. 8, pp. 1743–1761, 2015.

[27] Q. Qin, J. Q. Li, Y. G. Yue, and C. Y. Liu, "An adaptive and time-efficient ECG R-peak detection algorithm," *J. Healthcare Eng.*, vol. 2017, pp. 1–14, Sep. 2017.

[28] T. De Cooman *et al.*, "Heart beat detection in multimodal data using automatic relevant signal detection," *Physiol. Meas.*, vol. 36, no. 8, pp. 1691–1704, 2015.

[29] D. Pandit *et al.*, "A lightweight QRS detector for single lead ECG signals using a max-min difference algorithm," *Comput. Methods Programs Biomed.*, vol. 144, no. 6, pp. 61–75, 2017.

[30] R. Gutierrez-Rivas, J. J. García, W. P. Marnane, and Á. Hernandez, "Novel real-time low-complexity QRS complex detector based on adaptive thresholding," *IEEE Sensor J.*, vol. 15, no. 10, pp. 6036–6043, Oct. 2015.

[31] F. Plesinger, P. Klimes, J. Halamek, and P. Jurak, "Taming of the monitors: Reducing false alarms in intensive care units," *Physiol. Meas.*, vol. 37, no. 8, pp. 1313–1325, 2016.

[32] A. E. Johnson, J. Behar, F. Andreotti, G. D. Clifford, and J. Oster, "Multimodal heart beat detection using signal quality indices," *Physiol. Meas.*, vol. 36, no. 8, pp. 1665–1677, 2015.

[33] H. Khamis *et al.*, "QRS detection algorithm for telehealth electrocardiogram recordings," *IEEE Trans. Biomed. Eng.*, vol. 63, no. 7, pp. 1377–1388, Jul. 2016.

[34] M. Chan, D. Estève, J.-Y. Fourniols, C. Escriba, and E. Campo, "Smart wearable systems: Current status and future challenges," *Artif. Intell. Med.*, vol. 56, no. 3, pp. 137–156, 2012.

[35] D. Hayn, B. Jammerbund, and G. Schreier, "QRS detection based ECG quality assessment," *Physiol. Meas.*, vol. 33, no. 9, pp. 1449–1461, 2012.

[36] J. Behar, J. Oster, Q. Li, and G. D. Clifford, "ECG signal quality during arrhythmia and its application to false alarm reduction," *IEEE Trans. Biomed. Eng.*, vol. 60, no. 6, pp. 1660–1666, Jun. 2013.

[37] Q. Li, R. G. Mark, and G. D. Clifford, "Robust heart rate estimation from multiple asynchronous noisy sources using signal quality indices and a Kalman filter," *Physiol. Meas.*, vol. 29, no. 1, pp. 15–32, 2008.

[38] H. Naseri and M. R. Homaeinezhad, "Electrocardiogram signal quality assessment using an artificially reconstructed target lead," *Comput. Methods Biomech. Biomed. Eng.*, vol. 18, no. 10, pp. 1126–1141, 2015.

[39] C. Y. Liu *et al.*, "A multi-step method with signal quality assessment and fine-tuning procedure to locate maternal and fetal QRS complexes from abdominal ECG recordings," *Physiol. Meas.*, vol. 35, no. 8, pp. 1665–1683, 2014.

[40] J. S. Richman and J. R. Moorman, "Physiological time-series analysis using approximate entropy and sample entropy," *Amer. J. Physiol. Heart Circulatory Physiol.*, vol. 278, no. 6, pp. H2039–H2049, 2000.

[41] S. H. Wang *et al.*, "Identification of alcoholism based on wavelet Renyi entropy and three-segment encoded Jaya algorithm," *Complexity*, vol. 2018, pp. 1–13, Jan. 2018.

[42] C. Y. Liu and L. N. Zhao, "Using fuzzy measure entropy to improve the stability of traditional entropy measures," in *Proc. Comput. Cardiol.*, Hangzhou, China, 2011, pp. 681–684.

[43] L. N. Zhao *et al.*, "Determination of sample entropy and fuzzy measure entropy parameters for distinguishing congestive heart failure from normal sinus rhythm subjects," *Entropy*, vol. 17, no. 9, pp. 6270–6288, 2015.

[44] C. Y. Liu *et al.*, "Analysis of heart rate variability using fuzzy measure entropy," *Comput. Biol. Med.*, vol. 43, no. 2, pp. 100–108, 2013.

[45] Y. T. Zhang, S. S. Wei, C. Di Maria, and C. Y. Liu, "Using Lempel–Ziv complexity to assess ECG signal quality," *J. Med. Biol. Eng.*, vol. 36, no. 5, pp. 625–634, 2016.

[46] Y. T. Zhang, S. S. Wei, H. Liu, L. N. Zhao, and C. Y. Liu, "A novel encoding Lempel–Ziv complexity algorithm for quantifying the irregularity of physiological time series," *Comput. Methods Programs Biomed.*, vol. 133, no. 9, pp. 7–15, 2016.

[47] G. B. Moody, B. Moody, and I. Silva, "Robust detection of heart beats in multimodal data: The PhysioNet/computing in cardiology challenge 2014," in *Proc. Comput. Cardiol.*, Cambridge, MA, USA, 2014, pp. 549–552.

[48] C.-C. Chang and C. J. Lin, "LIBSVM: A library for support vector machines," *ACM Trans. Intell. Syst. Technol.*, vol. 2, no. 3, pp. 1–27, 2011.

[49] Y. D. Zhang, S. H. Wang, P. Phillips, and G. L. Ji, "Binary PSO with mutation operator for feature selection using decision tree applied to spam detection," *Knowl. Syst.*, vol. 64, no. 7, pp. 22–31, Jul. 2014.

[50] M. Weder *et al.*, "Embroidered electrode with silver/titanium coating for long-term ECG monitoring," *Sensors*, vol. 15, no. 1, pp. 1750–1759, 2015.

[51] J. P. S. Cunha *et al.*, "Vital-Jacket®: A wearable wireless vital signs monitor for patients' mobility in cardiology and sports," in *Proc. PervasiveHealth*, Munich, Germany, 2010, pp. 1–2.

[52] F. Miao, Y. Y. Cheng, Y. He, Q. Y. He, and Y. Li, "A wearable context-aware ECG monitoring system integrated with built-in kinematic sensors of the smartphone," *Sensors*, vol. 15, no. 5, pp. 11465–11484, 2015.

[53] S. Patel, H. Park, P. Bonato, L. Chan, and M. Rodgers, "A review of wearable sensors and systems with application in rehabilitation," *J. NeuroEng. Rehabil.*, vol. 9, no. 1, pp. 1–17, 2012.

Chengyu Liu (M'13) received the B.S. and Ph.D. degrees in biomedical engineering from Shandong University, Jinan, China, in 2005 and 2010, respectively.

He was a Post-Doctoral Fellow with Shandong University, from 2010 to 2013, Newcastle University, Newcastle upon Tyne, U.K., from 2013 to 2014, and Emory University, Atlanta, GA, USA, from 2015 to 2017. He is currently a Professor with the School of Instrument Science and Engineering, Southeast University, Nanjing, China. He is also the Director of the Southeast-Lenovo Wearable Heart-Sleep-Emotion Intelligent Monitoring Laboratory. He has authored or co-authored over 130 papers. His current research interests include mHealth and intelligent monitoring, machine learning and big data processing for cardiovascular signals, device development for CADs, and sleep and emotion monitoring.

Dr. Liu was the PI on 10+ awarded grants. He is currently a Federation Journal Committee member of International Federation for Medical and Biological Engineering and the Chair for China Physiological Signal Challenge 2018.

Xiangyu Zhang received the B.S. degree in measurement and control technology and instrument from the School of Mechanical Engineering, Southwest Jiaotong University, Chengdu, China, in 2014. He is currently pursuing the Ph.D. degree in instrument science and technology at Southeast University, Nanjing, China.

His current research interests include ECG signal processing, machine learning and deep learning, and body sensor networks.

Lina Zhao received the B.S. and M.S. degrees in biomedical engineering from Shandong University, Jinan, China, in 2005 and 2008, respectively, where she is currently pursuing the Ph.D. degree at the School of Control Science and Engineering.

She was a Researcher with Shandong Heng-Xin Inspection Technique Exploiture Center, Jinan. Her current research interests include entropy methods for physiological signal analysis, electrocardiogram, PCG, and artery pressure pulse processing.

Feifei Liu received the B.S. and Ph.D. degrees in biomedical engineering from Shandong University, Jinan, China, in 2010 and 2015, respectively.

She was a Post-Doctoral Fellow with Shandong University, from 2015 to 2017. She is currently a Post-Doctoral Fellow with Southeast University, Nanjing, China. She has authored or co-authored eight original journal/conference papers. Her current research interests include ECG signal processing, machine learning, and big data processing for physiological signals.

Xingwen Chen received the B.S. and M.S. degrees in electrical engineering and the minor degree in international economics and trade from the Harbin Institute of Technology, Harbin, China, in 2001 and 2003, respectively.

He also holds a PMP authentication. He is currently a Research and Development Director and a Senior Engineer with the Lenovo Empowerment Centre, Shenzhen, China. His current research interests include new sensors and material, wearable ECG device, wireless technology, smart device including smart wearable, smart home, and healthcare devices.

Yingjia Yao received the M.B.A. degree from the China Europe International Business School, Shanghai, China, in 2006.

In 1996, he joined Lenovo, Beijing, China, where he is currently the Vice President of the Lenovo Group, the General Manager of the Lenovo Empowerment Center, and the Chief Design Officer of the Lenovo Group. He established and has led the Lenovo Innovation Design Center in successfully delivering lots of leading product experience solutions. He currently leads the Lenovo Empowerment Center and Smart Lifestyle Innovation and Incubation Center with Lenovo Research.

Mr. Yao and his team won the Design Contest for the 2008 Beijing Olympic Torch.

Jianqing Li (M'06) received the B.S. and M.S. degrees in automatic technology from the School of Instrument Science and Engineering, Southeast University, Nanjing, China, in 1986 and 1992, respectively, and the Ph.D. degree in measurement technology and instruments from Southeast University.

He is currently a Professor with the School of Basic Medical Sciences, Nanjing Medical University, Nanjing, China, where he also acts as the Vice President. He is also a Professor with the School of Instrument Science and Engineering, Southeast University. His current research interests include mHealth, wearable electrocardiogram systems, multiparameter physiological signal detection, and wireless networks.